

Nonlinear dynamics of thermoacoustic instability using a kinematic, premixed flame model

N. Karimi, M.J. Brear and S.H. Jin

Department of Mechanical and Manufacturing Engineering,
University of Melbourne, Parkville, 3010, Australia

Abstract

This paper considers a simple, nonlinear model of a ducted laminar flame. Ducted flames are susceptible to thermoacoustic instability, in which perturbations in the flame heat release drive acoustic modes of the duct that, in turn, drive the flame perturbations. Both the forced response of the flame and the self-excited response of system are studied numerically. The form of the self-excited system behaviour is found to be strongly dependent on both the flame position and duct length. In particular, two basic forms of unstable behaviour are observed, in which the system either experiences a limit cycle or where the flame flashes back. These two responses feature very different time histories in heat release rate. This final result infers that the use of a saturation element to model the flame non-linearity is inappropriate.

Introduction

Thermoacoustic instability in different systems has been studied extensively over the last fifty or so years [1, 2]. During this time, the applications have varied a great deal, and include solid and liquid fuelled rockets, ramjets, gas turbines and industrial burners. Nonetheless, the essential mechanisms of this instability are the same in all these cases and feature a coupling between the unsteady heat release and the chamber acoustics. In recent years, environmental concerns regarding NO_x emissions have created considerable interest in the use of premixed flames in natural gas fired gas turbines. Due to the sensitivity of premixed flames to imposed velocity fluctuations, combustion instabilities have appeared again as a problem of considerable practical importance, and have spawned significant research effort world-wide.

Central to the contemporary problem of understanding thermoacoustic instability is the development of accurate and practical *predictive* tools for determining both the stability and (if unstable) the steady-state amplitude of the fluctuations in a given system. This is being approached in, effectively, two ways. The first is to attempt to model the physics of the problem directly with accurate numerical models of combustion in premixed flames. This typically involves LES or DNS codes with simplified reaction kinetics, and has the benefit of the model being more physically representative but also has the drawback of being computationally intensive [2]. Such approaches, whilst potentially accurate, are therefore not truly practical design tools at the moment since the designer often needs to perform parametric studies before settling on a final design.

An alternative approach is to develop simple models of the flame, the duct acoustics and their interaction. For example, the widely-observed sensitivity of premixed flames to low frequency disturbances, and their relative insensitivity to high frequency disturbances, has lead to several investigators modelling the flame as a kind of linear, low-pass filter [1-5]. The duct acoustics are then usually assumed to be linear and one-dimensional, thereby completing the model. Of course, such models only

address the linear stability of the system. More complex models are required to study the nonlinear dynamics.

Following this simple approach, the next level of sophistication that can capture a form of flame nonlinearity is usually to replace the dynamic model of the flame with a kinematic flame model [1, 4, 5]. These models typically consider the flame motion and heat release to be determined only by the local burning velocity and the axial velocity upstream of the flame. Importantly, the effects of vorticity, which is either transported into the flame or created by the flame itself, is not usually modelled. Whilst not studied in this paper, the authors consider that this omission is one of the main shortcomings of such models.

Dowling [3] makes the further claim that a linear dynamic model, combined with a saturation element, models the nonlinear flame dynamics reasonably. The saturation limits of the flame heat release rate are zero when the instantaneous velocity just upstream of the flame is less than or equal to zero, and twice the mean heat release rate when this instantaneous velocity is greater than twice the mean duct velocity. In her later paper that uses a kinematic flame model, Dowling [4] states that her prior use of this saturation element is reasonable, but in the present authors' view, does not verify this rigorously.

The dynamics of such models is relatively easy to analyse using numerical software such as Matlab/Simulink. However, any practical benefit in their speed must be weighed up against their inevitably diminished accuracy. Furthermore, whilst these models are relatively common in the literature, the authors consider that their accuracy has not been clearly established. It is therefore not presently clear where in this broad range of modelling choices, from 'slow and more accurate' LES/DNS to 'fast and less accurate' simple models, that a practical and accurate predictive tool actually lies.

This paper is therefore part of the authors' overall, longer-term aim to determine the requirements for *accurate and practical* predictive tools for studying thermoacoustic instability. The paper is concerned first with Dowling's [4] kinematic flame model applied to a ducted, laminar, premixed flame, and combines this with a simple model of the duct acoustics that was first presented by Dowling in [3]. Two basic forms of unstable behaviour are observed, in which the system either goes into a limit cycle, or where the flame flashes back. These two responses feature very different time histories in heat release rate. As such, they cannot in general be modelled using a simple saturation element integrated into a linear model as Dowling [3] argued.

Model

Flame model

Figure 1 shows a schematic diagram of the present problem. The flame is stabilised behind a flame holder of radius $a = 17.5 \text{ mm}$, the end of which is referred to as the gutter, and extends to the duct wall of radius $b = 35 \text{ mm}$. The duct has uniform cross-section and open upstream and downstream boundaries. The duct

velocity $u(x,t)$ is assumed uniform across the duct and purely axial with mean $\bar{u}=1.0\text{ m/s}$. Given the low Mach number of the upstream flow and assuming that the flame holder is acoustically compact, the velocity at the gutter $u_g(t)$ is related to the duct velocity just upstream of the flame holder by continuity

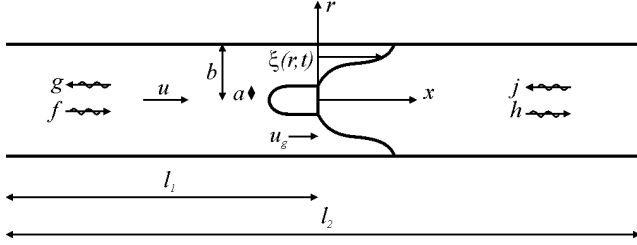
$$u_g(t) = u(0,t)/(1 - a^2/b^2). \quad (1)$$


Figure 1: Schematic of the flame, flame holder and duct.

The present geometry is axisymmetric, and it is assumed that combustion occurs within a thin sheet whose instantaneous position $\xi(r,t)$ is a function of radius and time only. The flame surface is therefore described by another function $G(x,r,t)=0$, such that

$$G(x,r,t) = x - \xi(r,t). \quad (2)$$

The flame surface propagates with a speed $(\underline{u} \cdot \hat{n} - S_L)$ in the direction of its surface normal \hat{n} , where S_L is the laminar flame speed. It is assumed that $S_L = 0.4\text{ m/s}$ for an ethylene/air mixture with an equivalence ratio $\phi = 0.7$ [6]. The propagation of the surface $G(x,r,t)=0$ is therefore described by the well-known ‘G equation’ [1, 2, 4, 5],

$$\frac{\partial G}{\partial t} + \underline{u} \cdot \nabla G = S_L |\nabla G|. \quad (3)$$

Dowling [4] and Fleifil et al. [5] both argue that the vertical component of the flow velocity vector is negligible at the flame surface. Accepting their arguments, combination of equations (2) and (3) gives a nonlinear PDE for the flame position

$$\frac{\partial \xi}{\partial t} = u_g - S_L \sqrt{1 + (\partial \xi / \partial r)^2}. \quad (4)$$

It is noted that this expression models the axial velocity just upstream of the flame as equal to the gutter velocity u_g . This assumes that the flame is compact relative to the duct acoustics, which is reasonable in most cases.

Boundary conditions for equation (4) are quite involved since there is a possibility that the flame surface will flash back when the flow velocity is less than burning velocity. It is also assumed that the flame cannot blow out. Boundary conditions that incorporates these considerations are

$$\xi(a,t) = 0 \quad (5)$$

if $\xi(a,t^-) = 0$ and $u_g(t) \geq S_L$, and

$$(\partial \xi / \partial r)_{r=a} = u_g - S_L \quad (6)$$

otherwise. The initial condition for the simulations is the average surface position $\bar{\xi}(r)$, which can easily be shown from equation (4) to be a truncated cone that extends from the gutter to the duct wall

$$\bar{\xi}(r) = (r - a) \sqrt{u_g^2 - S_L^2} / S_L. \quad (7)$$

Equation (4) was integrated using a 2nd order accurate spatial difference for $\partial \xi / \partial r$ and fourth-order Runge-Kutta timestepping for obtaining ξ from $\partial \xi / \partial t$. The spatial resolution was 0.09 mm and the timestep was $100\text{ }\mu\text{s}$, which were found to give solutions that were independent of both the spatial and temporal discretisation.

The instantaneous flame surface area is

$$A(t) = 2\pi \int_a^b r \sqrt{1 + (\partial \xi / \partial r)^2} dr \quad (8)$$

and the heat release rate $Q(W)$ is

$$Q(t) = \eta \rho_u S_L \Delta H_R A(t), \quad (9)$$

where $\eta = 0.8$ is a combustion efficiency, ρ_u is the density of the reactants (1.2 kg/m^3) and ΔH_R is the enthalpy of reaction, which for an ethylene/air mixture with $\phi = 0.7$ was set to $2.14\text{ MJ/kg}_{mixture}$ [6].

For linear, harmonic perturbations of frequency ω , Dowling [4] also solves equation (4) analytically, and integrates it across the duct to obtain the dynamic response of the complex, overall heat release perturbations \hat{Q} to imposed complex, velocity perturbations \hat{u}_g at the gutter,

$$\frac{\hat{Q} / \bar{Q}}{\hat{u}_g / \bar{u}_g} = \frac{2}{i\Omega(a+b)} \left[a - b e^{-i\Omega} + \frac{(b-a)}{i\Omega} (1 - e^{-i\Omega}) \right]. \quad (10)$$

The corresponding real perturbations are given by $Q' = \text{Re}(\hat{Q} e^{j\omega t})$ and $u'_g = \text{Re}(\hat{u}_g e^{j\omega t})$ with mean values \bar{Q} and \bar{u}_g . The term Ω is a Strouhal number, defined by

$$\Omega = \omega(b-a) / S_L \sqrt{1 - (S_L / \bar{u}_g)^2}.$$

Duct acoustics model

Figure 1 also shows acoustic waves

$$\begin{aligned} p'(x,t) &= f(t - x/(\bar{c}_1 + \bar{u}_1)) + g(t + x/(\bar{c}_1 - \bar{u}_1)), \\ u'(x,t) &= [f(x,t) - g(x,t)] / (\bar{\rho}_1 \bar{c}_1), \end{aligned} \quad (11)$$

upstream of the flame (region 1 i.e. $x < 0$) and

$$\begin{aligned} p'(x,t) &= h(t - x/(\bar{c}_2 + \bar{u}_2)) + j(t + x/(\bar{c}_2 - \bar{u}_2)), \\ u'(x,t) &= [h(x,t) - j(x,t)] / (\bar{\rho}_2 \bar{c}_2), \end{aligned} \quad (12)$$

downstream (region 2 i.e. $x > 0$), where \bar{c} is the mean sonic velocity (m/s). The flame also produces entropy fluctuations, but as the duct exit is open, these convect out of the domain without having any (first order) effect on the duct pressure and velocity, and so are neglected.

Application of the condition that $p' = 0$ at the upstream and downstream boundaries gives

$$\begin{aligned} f(0,t) &= -g(0,t - \tau_u), \\ j(0,t) &= -h(0,t - \tau_d). \end{aligned} \quad (13)$$

The terms τ_u and τ_d are time lags that represent the time taken for a wave to travel from the flame, reflect from the upstream or downstream boundary and return to the flame:

$$\begin{aligned} \tau_u &= 2l_1 / [\bar{c}_1 (1 - \bar{M}_1^2)], \\ \tau_d &= 2(l_2 - l_1) / [\bar{c}_2 (1 - \bar{M}_2^2)], \end{aligned} \quad (14)$$

where \bar{M} is the mean Mach number in that region.

Dowling [3] combines equations (13) and (14) with the equations for mass, momentum and energy conservation applied across the (assumed acoustically compact) flame to obtain the following matrix equation

$$\mathbf{X} \begin{pmatrix} g(0,t) \\ h(0,t) \end{pmatrix} = \mathbf{Y} \begin{pmatrix} g(0,t-\tau_u) \\ h(0,t-\tau_d) \end{pmatrix} + \begin{pmatrix} 0 \\ (Q(t)-\bar{Q})/\pi b^2 \bar{c}_1 \end{pmatrix}, \quad (15)$$

where matrices \mathbf{X} and \mathbf{Y} are given in the appendix. Solving equations (15), (11), (12) and (1) for the velocity perturbation at the flame, the instantaneous heat release in equation (9) can then be determined by the numerical integration of equation (4), thereby closing the integrated model of the flame and the duct acoustics.

Results and discussion

Figure 2 shows the steady state flame response to sinusoidal velocity forcing (i.e. ignoring the duct acoustics) with an amplitude of 1% of the mean velocity. The numerical simulation's amplitude and phase responses were calculated by least-squares curve fitting a sinusoid with the same frequency as the excitation to the observed, closely sinusoidal response. As expected, the simulations are in close agreement with the linear, analytic dynamic response given by equation (10). The commonly reported [1-5] behaviour of the flame as a kind of low-pass filter to small amplitude excitation is also clear.

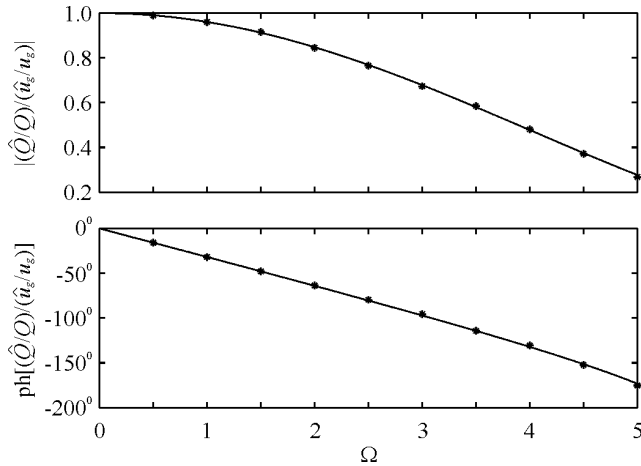


Figure 2: Dynamic response of the flame (solid line: equation (10), points: nonlinear simulations with $|u'_g/\bar{u}_g| = 0.01$).

Figure 3 shows the variations in the heat release, gutter velocity and gutter pressure with time for the integrated flame/acoustic model, for a duct length l_2 of 1.0 m and the gutter placed at $l_1 = 0.6$ m. The system can be seen to undergo at first a roughly exponential, self-excited disturbance growth in all three quantities until it settles into a constant amplitude limit cycle. The frequency and growth rate of the oscillations during the period of disturbance growth should correspond closely to the unstable duct modes predicted by a linear stability analysis of the system using equation (10) e.g. [7].

The time traces in Figure 3 show relatively small amplitude limit cycle fluctuations in the static pressure, but appreciable velocity fluctuations. Dowling [3] explains this behaviour by noting that since $u' \sim O(p'/\rho c)$ in equation (11), it follows from the ideal gas law that

$$p'/\bar{p} \sim O(u'\bar{\rho c}/\bar{p}) = O(\gamma \bar{M} u'/\bar{u}). \quad (16)$$

Thus, the fractional pressure fluctuations remain small in a low Mach number flow even when $u'/\bar{u} \sim O(1)$. The flame heat release fluctuations are also relatively small. Animations show

that the flame remains anchored at the gutter, oscillating around its undisturbed position given by equation (7).

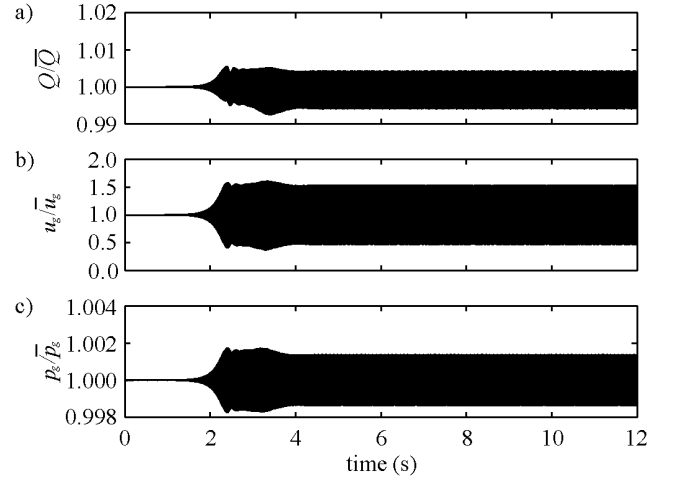


Figure 3: Time series of a) Q/\bar{Q} , b) u_g/\bar{u}_g and c) p_g/\bar{p}_g for $l_1 = 0.6$ m and $l_2 = 1.0$ m.

Figure 4 shows that very different behaviour is observed when the length of the duct and gutter position are doubled ($l_2 = 2.0$ m, $l_1 = 1.2$ m). The pressure fluctuations remain relatively small, although larger than previously, but the velocity perturbations are now large enough that reversed flow is observed as part of the oscillation. Interestingly, the mean flame heat release departs from that given by equations (7), (8) and (9) and must be an inherently nonlinear effect.

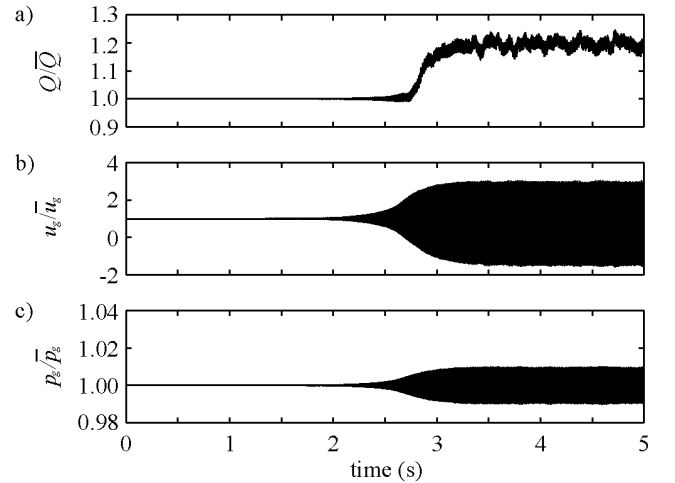


Figure 4: Time series of a) Q/\bar{Q} , b) u_g/\bar{u}_g and c) p_g/\bar{p}_g for $l_1 = 1.2$ m and $l_2 = 2.0$ m

Animations of the flame motion in this instance reveal that the flame is no longer anchored to the gutter, but instead progresses gradually upstream as it oscillates in response to the acoustic excitation (eg. Figure 5). This type of behaviour can be called 'flashback', and is a common problem in premixed combustors. A surprising but reasonable result in the present study is that the heat release fluctuation amplitude in Figure 4, which is dependent on the flame surface area, does not change greatly as the flame gradually moves upstream.

A criterion for determining when flame flashback occurs is not obvious, since it is related to both the amplitude and frequency of the acoustic forcing (Figure 5). Both the nonlinear numerical

simulations and linear theory showed that the flame heat release, which drives the duct acoustics, is relatively insensitive to high frequency excitation, regardless of the forcing amplitude. Thus, the flame tends to either limit cycle or flashback in longer ducts, where the fundamental acoustic mode of the duct is relatively low and hence more likely to drive significant flame motion and heat release perturbations (Figure 6).

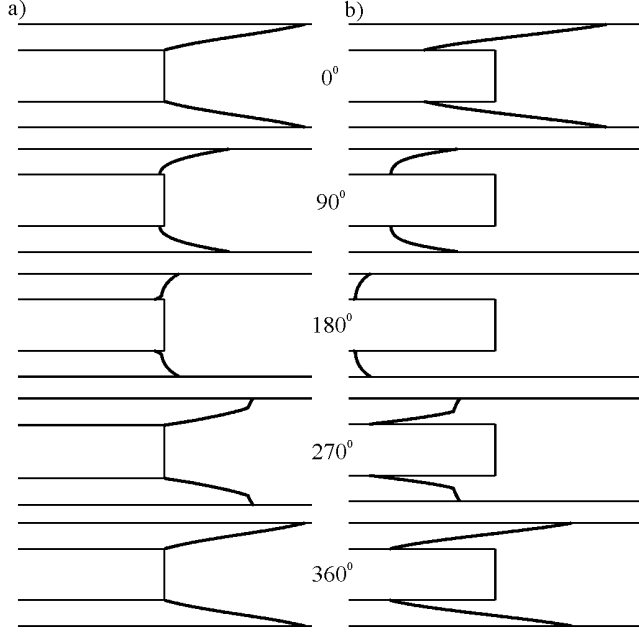


Figure 5: Instantaneous flame surface during steady state sinusoidal forcing, $\Omega = 2.5$ and a) $|u'_g / \bar{u}_g| = 1$, b) $|u'_g / \bar{u}_g| = 2$.

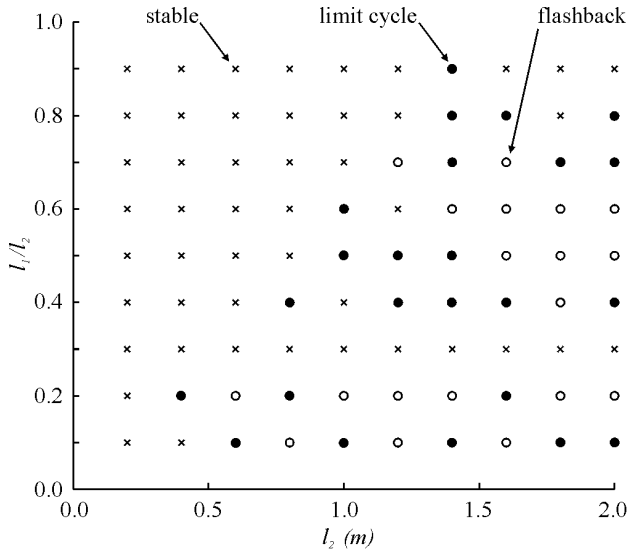


Figure 6: Stability map for different combinations of l_1 and l_2 .

The kinematic flame model predicted that the steady state amplitude of the heat release fluctuations during thermoacoustic instability of either form never exceeded roughly 10% of the mean heat release. Furthermore, Figure 3 and Figure 4 showed that the heat release fluctuation amplitude was strongly dependent on the form of unstable behaviour. Both these amplitudes are significantly smaller than that proposed by Dowling [3], who argued that heat release fluctuations of the same order as the mean heat release were reasonable. Indeed, the use of Dowling's [3] saturation limits and the linear model in equation (10), as Dowling suggests, were observed to cause excessive velocity perturbations in the duct, well in excess of any

predicted by the nonlinear, kinematic flame model. It is also not obvious how to determine *a priori* whether the flame flashes back or goes into limit cycle given knowledge only of the duct's mean flow. Thus, this range of possible nonlinear responses cannot in general be modelled using a linear flame model with saturation as Dowling [3] argued.

Conclusions

This paper presented an analysis of an integrated kinematic model of a ducted, laminar, premixed flame combined with a simple model of the duct acoustics. Depending on the system parameters, two basic forms of unstable behaviour were observed. The flame either maintained its position around its stabilisation point on the flame holder, in which case the acoustic velocity perturbations excited by the flame were relatively small, or the flame 'flashed back' by moving upstream of the flame holder. This latter response featured significantly larger duct velocity perturbations and periods of reversed duct flow.

In both cases, the kinematic flame model predicted that the steady state amplitude of the heat release fluctuations was significantly smaller than that suggested by Dowling [3] as a reasonable saturation limit for this instability. It is also not obvious how to determine *a priori* whether the flame flashes back or goes into limit cycle given knowledge only of the duct's mean flow. Thus, the range of observed nonlinear responses cannot in general be modelled using a linear flame model with saturation as Dowling [3] argued.

References

1. Lieuwen, T., *Modeling premixed combustion - acoustic wave interactions: a review*. Journal of Propulsion and Power, 2003. **19**(5): p. 765-781.
2. Candel, S. *Combustion dynamics and control: progress and challenges*. in *Proceedings of the Combustion Institute*. 2002.
3. Dowling, A.P., *Non-linear self excited oscillations of a ducted flame*. Journal of Fluid Mechanics, 1997. **346**: p. 271-290.
4. Dowling, A.P., *A kinematic model of a ducted flame*. Journal of Fluid Mechanics, 1999. **394**: p. 51-72.
5. Fleifil, M., Annaswamy, A.M., Ghoniem, Z. and Ghoniem, A.F., *Response of a laminar premixed flame to flow oscillations: A kinematic model and thermoacoustic instability results*. Combustion and Flame, 1996. **106**: p. 487-510.
6. Glassman, I., *Combustion*. 3rd ed. 1996: Academic Press, San Diego, California.
7. Hield, P.A., Brear, M.J. and Moase, W. *A parametric, linear stability analysis of thermoacoustic oscillation*. in *2003 Australian Symposium on Combustion*. 2003. Monash University: Monash University.

Appendix

The matrices in equation (15) are

$$\mathbf{X} = \begin{bmatrix} -1 + \bar{M}_1 \left(2 - \frac{\bar{u}_2}{\bar{u}_1} \right) - \bar{M}_1^2 \left(1 - \frac{\bar{u}_2}{\bar{u}_1} \right) & 1 + \bar{M}_1 \frac{\bar{\rho}_1 \bar{c}_1}{\bar{\rho}_2 \bar{c}_2} \\ \frac{1 - \gamma \bar{M}_1}{\gamma - 1} + \bar{M}_1^2 - \bar{M}_1^2 (1 - \bar{M}_1) \frac{1}{2} \left(\frac{\bar{u}_2^2}{\bar{u}_1^2} - 1 \right) & \frac{\bar{c}_2 (1 + \gamma \bar{M}_2)}{\bar{c}_1 (\gamma - 1)} + \bar{M}_1 \bar{M}_2 \frac{\bar{\rho}_1}{\bar{\rho}_2} \end{bmatrix}$$

$$\mathbf{Y} = \begin{bmatrix} - \left[1 + \bar{M}_1 \left(2 - \frac{\bar{u}_2}{\bar{u}_1} \right) + \bar{M}_1^2 \left(1 - \frac{\bar{u}_2}{\bar{u}_1} \right) \right] & 1 - \bar{M}_1 \frac{\bar{\rho}_1 \bar{c}_1}{\bar{\rho}_2 \bar{c}_2} \\ - \left[\frac{1 + \gamma \bar{M}_1}{\gamma - 1} + \bar{M}_1^2 - \bar{M}_1^2 (1 + \bar{M}_1) \frac{1}{2} \left(\frac{\bar{u}_2^2}{\bar{u}_1^2} - 1 \right) \right] & - \frac{\bar{c}_2 (1 - \gamma \bar{M}_2)}{\bar{c}_1 (\gamma - 1)} - \bar{M}_1 \bar{M}_2 \frac{\bar{\rho}_1}{\bar{\rho}_2} \end{bmatrix}$$